

Marjoram Oil Attenuates Valproic Acid-Induced Pancreatic Damage in Adult Male Albino Rats: A Histological and Immunohistochemical Study

Amira Adly Kassab, Heba EM Sharaf Eldin and Amal AA Abd-El-Hafez

Department of Histology and Cell Biology, Faculty of Medicine, Tanta University, Egypt

ABSTRACT

Introduction: Valproic acid [VA] is an antiepileptic drug that is extensively prescribed for many neurological disorders. Its use is associated with serious pancreatic complications. Marjoram oil [MO] is a health protective agent with proved anti-oxidant activity.

Aim: Study of the effect of valproic acid on pancreas of adult male albino rats exploring novel mechanisms of VA-induced pancreatic damage and to evaluate the potential protective role of marjoram oil.

Materials and Methods: Fifty adult male albino rats were used as a control group, a valproic acid group and a valproic acid-marjoram group. Both VA [200mg/kg] and MO [0.5ml/kg] were given once a day orally for eight weeks. Specimens of the pancreas were processed for light and electron microscopic studies. Immunohistochemical study was performed using anti-P53 antibodies.

Results: Specimens of the valproic acid group showed an obvious distortion in the pancreatic acini as well as the islets of Langerhans. The acinar and islets cells showed cytoplasmic vacuoles and pyknotic nuclei. Large autophagic vacuoles containing an acidophilic material appeared in many cells. Dilated ducts and blood vessels were seen. There was a significant increase in the P53-immunoreaction of the acinar and islets cells and a significant decrease in the number of the zymogen granules of the acinar cells. Ultrastructurally, there were shrunken nuclei with irregularity, dilated rough endoplasmic reticulum and swollen mitochondria in the acinar cells and beta cells. In contrast, minimal changes occurred in the valproic acid-marjoram group that received MO before VA.

Conclusion: Valproic acid administration to albino rats resulted in significant structural alterations in the pancreas. Marjoram oil attenuated VA effect and preserved the pancreas structure.

Received: 08 January 2021, **Accepted:** 07 February 2021

Key Words: Electron microscopy, immunohistochemistry, marjoram oil, pancreas, valproic acid.

Corresponding Author: Amira A. kassab, MD, Department of Histology and Cell Biology, Faculty of Medicine, Tanta University, Egypt, **Tel.:** +20 10 1669 7635, **E-mail:** Amirakassab80@yahoo.com

ISSN: 1110-0559, Vol. 45, No. 3

INTRODUCTION

Valproic acid (VA) and its salts, mainly sodium valproate, are effective antiepileptic and anticonvulsant drugs^[1]. It was approved by Food and Drug Administration since 1978^[2]. Valproic acid is well established in the treatment of childhood epilepsy^[3]. Although, it is also widely prescribed in the treatment of adult epilepsy, bipolar disorder, anorexia nervosa, panic attack, anxiety disorder, migraine and as a mood stabilizer^[4,5].

Despite of VA is well tolerated at therapeutic doses; it has inherent toxicity^[6]. It had been reported that VA induced neurotoxicity^[7], hepatotoxicity^[3], hematotoxicity^[8], nephrotoxicity^[9], testicular damage^[10], teratogenicity^[11] as well as pancreatitis^[12].

Acute pancreatitis is one of the most severe VA-related toxicity^[1]. Valproic acid induced-pancreatitis might be an idiosyncratic complication^[2], or dose-dependent toxicity^[13]. Outcomes for patients with VA-associated pancreatitis have ranged from full recovery after discontinuation of the drug to severe hemorrhagic pancreatitis and death^[14].

The mechanism of VA-induced acute pancreatitis has not been fully elucidated^[13]. Yet, it had been reported that VA stimulates depletion of antioxidant enzymes resulting in increasing in the intracellular reactive oxygen species (ROS)^[15]. Elevated ROS levels induce pancreatitis via direct toxic effect on the cell membranes of the pancreatic cells^[16]. However, it was claimed that VA does not directly cause pancreatitis but inhibits histone deacetylase (HDAC) which controls acinar cell proliferation affecting the pancreatic regenerative capacity and causing delay in the pancreatic healing^[17].

Nowadays, world gives a special attention to medicinal and aromatic plants as an efficient source of bioactive agents for maintaining health and preventing diseases. One of these aromatic plants is Marjoram (*Origanum majorana* L) which belongs to Lamiaceae family, a herbaceous and perennial plant native to southern Europe and the Mediterranean^[18,19]. Marjoram is a kitchen herb and is used as oil in food processing, flavoring and other culinary purposes^[20]. Additionally, Marjoram oil is known to have a high curative effect in traditional and herbal medicine.

It is used in cases of chest infection, cough, sore throat, rheumatic pain, nervous disorders, cardiovascular diseases, epilepsy, insomnia, skin care, latulence, and stomach disorders^[21,22].

Marjoram oil is considered as an antiseptic, antidiabetic, carminative, antispasmodic, stimulant, diaphoretic and diuretic agent^[23]. Furthermore, Marjoram oil is known as a potent anti-oxidant due to its high polyphenolic contents^[24]. Previous studies revealed the protective effect of marjoram oil against liver toxicity^[25] and on the antioxidant enzymes in diabetic rats^[26].

From the previous data, we are much interested to do this scientific work that aimed to study the effect of valproic acid on pancreas of adult male albino rats exploring novel mechanisms of VA-induced damage and to evaluate the potential protective role of marjoram oil through varied histological methods.

MATERIALS AND METHODS

Ethical approval

The study procedures were performed in the Histology Department at Tanta Faculty of Medicine, Egypt. The experiment steps were carried out according to the animal use guidelines in scientific research accepted by the Local Ethics Committee of Tanta Faculty of Medicine, Egypt {Approval code: 32660/10/18}.

Chemicals

1. Valproic acid sodium salt: It is a white crystalline powder {100gm in a glass bottle} which was obtained from Sigma-Aldrich Co. {CAS Number: 1069-66-5}.
2. Marjoram oil: a glass bottle contains 30 ml of marjoram oil which is manufactured by El Captain Company {Cap Pharm, Egypt}.

Study design

Fifty male adult albino rats {200-270 grams} were used. They were continued on a standard 12-hours light and 12-hours dark cycles in properly ventilated clean cages before the experiment procedures and also throughout the experiment period with an access to balanced laboratory diet and water ad libitum. They were divided into three experimental groups:

(1) Group I (control group): Thirty rats were equally subdivided into three subgroups: the first {subgroup Ia} received no treatment, the second {subgroup Ib} received 1ml distilled water [the vehicle of valproic acid] orally once a day for 8 weeks and the third {subgroup Ic} received marjoram oil 0.5 ml/kg/day orally by a gastric tube once a day for 8 weeks^[27].

(2) Group II (valproic acid group): Ten rats received valproic acid at a dose of 200 mg/kg/day which was dissolved in 1ml distilled water. The solution was administered to rats orally by the gastric tube once a day

for 8 weeks^[28]. Oral route was selected in this study because it is the most commonly used route of administration of valproic acid in human.

(3) Group III (valproic acid-marjoram group): Ten rats received MO at 0.5 ml/kg/day, one hour before the valproic acid dose of 200 mg/kg/day orally by the gastric tube once a day for 8 weeks.

Tissue Sampling

At the end of the treatment period {8 weeks}, pentobarbital {50mg/kg} was injected intraperitoneally to anesthetize rats^[29]. The abdominal wall of all rats was incised along the entire length of the abdomen to open the abdominal cavity and to expose the viscera. Then, the pancreas was dissected out to take samples from the splenic segment to be processed for light and electron microscopic examination.

For light microscope (L/M)

Some of the pancreatic tissue samples were immediately fixed in 10% neutral-buffered formalin, washed, dehydrated, cleared and finally embedded in paraffin. Then, serial sections of 5µm thickness were stained with haematoxylin and eosin {H&E} stain to be visualized by L/M^[30].

For immunohistochemistry

Sections of the pancreatic tissue (5µm thickness) were deparaffinized, rehydrated, and rinsed in phosphate buffered saline. Then, the sections were incubated in a moist chamber with the primary antibody [rabbit polyclonal antibody against P53 protein, ab131442, Abcam, Cambridge, USA, 1:100 dilution] in phosphate buffered saline overnight at 4 °C. Thereafter, it was rinsed in the same buffer, and co-incubated for one hour with biotinylated secondary antibody {Dako North America, Inc., CA, USA} at the room temperature. Streptavidin peroxidase was added for ten minutes and washed three times in the phosphate buffered saline. The immunoreactivity was visualized using 3, 3'-diaminobenzidine [DAB]-hydrogen peroxide {a chromogen}. Finally, the slides were counterstained by Mayer's haematoxylin. The negative control sections were processed without increment of the primary antibody^[31]. Positive control for P53 was human breast carcinoma. All slides were evaluated in triplicates in order to confirm the accuracy of the results. The pancreatic cells with brown nuclear staining were considered as P53-immunopositive cells.

For electron microscope (E/M)

Processing of the pancreatic samples for transmission E/M was done according to the usual routine protocol. Small pieces of pancreatic tissues {1 mm³} were fixed in 2.5% phosphate-buffered glutaraldehyde at 4 °C for two hours then rinsed in phosphate buffered saline. After that, the pancreatic specimens were post-fixed in 1% prepared phosphate buffer osmium tetroxide at 4 °C for one hour.

Then, the pancreatic specimens were dehydrated in ascending grades of alcohol, immersed in propylene oxide, and finally embedded in the epoxy resin mixture. Semithin sections {1 μm thick} were cut, stained with toluidine blue, and examined by L/M to determine the suitable areas. Ultrathin sections {80–90 nm thick} were contrasted with uranyl acetate and lead citrate to be examined under JEOL-JEM-100 transmission E/M (JEOL, Tokyo, Japan). The pancreatic sample processing for E/M and photographing were carried out in the Electron Microscopy Unit, Tanta Faculty of Medicine, Egypt^[32].

Morphometric study

Images were taken by a Leica microscope {DM3000; Leica Microsystems, Wetzlar, Germany} joined to a CCD camera {DFC-290; Leica, Heerbrugg, Switzerland}. Image analysis was carried out utilizing a Leica Q-Win 500C image analyzer system {Leica Imaging System Ltd, Cambridge, UK} at the Central Research Lab, Tanta Faculty of Medicine, Egypt. Ten different non-overlapping fields were selected from each pancreatic specimen in each rat group and were examined to quantitatively evaluate:

1. Area percentage {area %} of the positive P53 immunoreaction of the pancreatic cells in each DAB-stained slide {at a magnification of X 400}.
2. The number of the zymogen granules in the ultrathin sections {at a magnification of X 2000}.

Statistical analysis

Data from the morphometric study were analyzed by one-way analysis of variance (ANOVA) followed by Tukey's procedure to compare between all rat groups employing the statistical package for social sciences software {version 11.5; SPSS Inc., Chicago, Illinois, USA}. The mean values as well as the standard deviation {Mean \pm SD} for each group were obtained. Probability value {*P* value} less than 0.05 was regarded as significant^[33].

RESULTS

All animals tolerated all experimental procedures and survived until the end of the treatment period.

Light microscopic findings

Group I (control group): All control subgroups showed similar histological features of the pancreas in H&E-stained sections. The examination revealed the characteristic lobular architecture of the pancreas consisting of many islets of Langerhans interspersed among the abundant exocrine acini. The islets were lightly stained than the surrounding acini. The exocrine acini had narrow lumen and were closely packed with very little connective tissue in-between. The acinar cells showed characteristic apical acidophilia and basal basophilia. Their nuclei were basal and rounded. Islets of Langerhans contained cords of lightly stained rounded or polygonal cells with blood capillaries in-between. The thin connective tissue septa between the pancreatic lobules contained variable sized

interlobular ducts and blood vessels. The ducts were lined by cuboidal epithelium (Figures 1,2).

Group II (valproic acid group): Examination of H&E stained sections of valproic acid treated rats revealed an obvious distortion in the exocrine acini and islets of Langerhans which was in the form of cellular degeneration with disturbed architecture of many pancreatic lobules. Cytoplasmic vacuolation and pyknotic nuclei were observed in many acinar and islets cells of the widely separated lobules. Many acinar cells showed large autophagic vacuoles containing acidophilic material. Some pancreatic lobules showed disturbed normal acinar architecture and heavy infiltration with mononuclear inflammatory cells that widely separated the acini from each other. An apparent decrease in the size and number of the acini as well as in the apical acidophilia of the acinar cells was observed. Dilated interlobular and intralobular ducts with retained secretion and flattening of their lining epithelium were noticed. The dilated ducts were surrounded by inflammatory cells. Markedly dilated and congested blood vessels with perivascular cellular infiltration were also seen (Figures 3,4,5,6).

Group III (valproic acid-marjoram group): This group showed preserved architecture of most pancreatic lobules with preserved morphological structure of most acinar and islets cells. The cells and their nuclei appeared more or less as the control ones. A few damaged acini were occasionally seen. Mild dilatation of the ducts and congestion of the blood vessels with minimal cellular infiltration were seen in focal areas (Figures 7,8).

Immunohistochemical findings

P53 immunostaining: P53-immunostained pancreatic sections of Group I (control group) displayed a weak positive nuclear reaction in a few acinar and islets cells. In Group II (valproic acid group), a strong positive nuclear reaction for P53 was detected in many acinar and islets cells, while in Group III (valproic acid-marjoram group), a moderate positive nuclear immunoreaction for P53 was observed in some acinar and islets cells (Figures 9,10,11)

Electron microscopic findings

Group I (control group): Ultrastructurally, the examination of all control subgroups revealed the normal structure of the acinar cells and islets cells. The acinar cells exhibited all the characteristic features of the protein synthesizing cells. In most sections, the acinar cells appeared pyramidal or polyhedral in shape and had a well defined polarity. Their apical cytoplasm was filled with spherical electron-dense secretory granules (zymogen granules) which were membrane bounded granules. The basal part of their cytoplasm contained rounded euchromatic nuclei which were surrounded with well-developed parallel cisternae of the rough endoplasmic reticulum and mitochondria. A few short microvilli from the apical cell membrane projected into the lumen of the acini. Moreover, the junctional complexes were seen between the lateral cell membranes of the acinar cells (Figure 12).

Considering the islets of Langerhans, the most detectable cells in all sections were beta and alpha cells. The beta cells were the most numerous cells and were concentrated mainly in the center of the islets while alpha cells were less numerous and were detected mainly in the periphery of the islets. The cytoplasm of beta cells contained numerous rounded secretory granules which were composed of an electron-dense core surrounded by a wide electron-lucent halo. A slightly ovoid regular nuclei, multiple mitochondria, rough endoplasmic reticulum and Golgi apparatus were also observed in the beta cell cytoplasm (Figure 13). The cytoplasm of alpha cells showed ovoid nuclei, numerous electron-dense granules, multiple mitochondria and rough endoplasmic reticulum (Figure 14).

Group II (valproic acid group): The ultrastructural examination of this group revealed obvious changes affecting mainly the acinar cells and beta cells. Dilated rough endoplasmic reticulum, dilated perinuclear space, swollen mitochondria with disrupted cristae and shrunken irregular heterochromatic nuclei were observed in many acinar cells. Deterioration of the normal polarity of the acinar cells was observed in most acini. Some cells showed abnormal distribution of the granules together with an apparent decrease in their number. Fusion of some granules was also seen. The content of these granules showed less electron density than the control ones (Figures 15,16).

Beta cells were also affected and showed cytoplasmic vacuoles, swollen disrupted mitochondria, dilated rough endoplasmic reticulum, dilated perinuclear space and numerous autophagic vacuoles. Moreover, the nuclei were shrunken and had irregular outlines with condensed chromatin (Figure 17). Regarding alpha cells, there were no observable ultrastructural changes in the cytoplasm or the nucleus (Figure 18).

Group III (valproic acid-marjoram group): This group showed preserved ultrastructure of most acinar and beta cells as well as alpha cells. The cytoplasmic organelles, the granules and the nuclei appeared more or less as the control ones. However, a few beta cells showed mild rough endoplasmic reticulum dilatation (Figures 19,20,21).

Morphometric and statistical results (Table 1, Histogram 1)

The area percentage of P53 immunoreaction of the pancreatic cells displayed a significant elevation in Group II (valproic acid group) compared to Group I. Furthermore, Group III (valproic acid-marjoram group) possessed a non-significant elevation compared to Group I.

Regarding the mean number of the zymogen granules of the acinar cells, the statistical values revealed a significant decrease in group II (valproic acid group) compare to group I, while no significant difference was detected in group III (valproic acid-marjoram group) compared to group I.

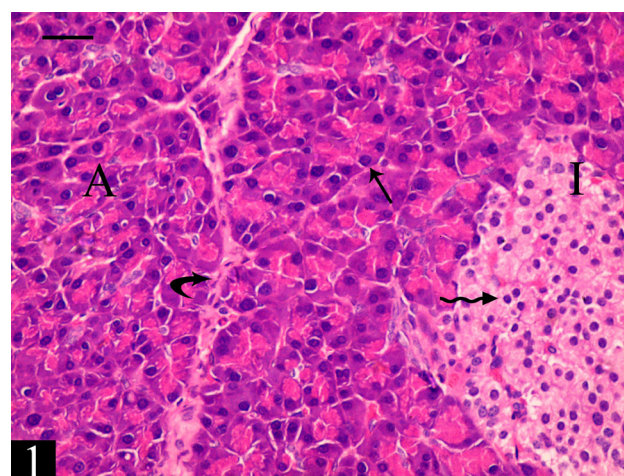


Fig. 1: showing numerous pancreatic acini (A) and a pale stained islets of Langerhans (I). The acinar cells show basal basophilia, apical acidophilia and rounded basal nuclei (arrow). The polygonal islets cells (wavy arrow) are arranged in cords with blood capillaries in-between. Notice thin connective tissue septa (curved arrow) between the pancreatic lobules. (Group I, H&E X 400, Scale bar = 50µm)

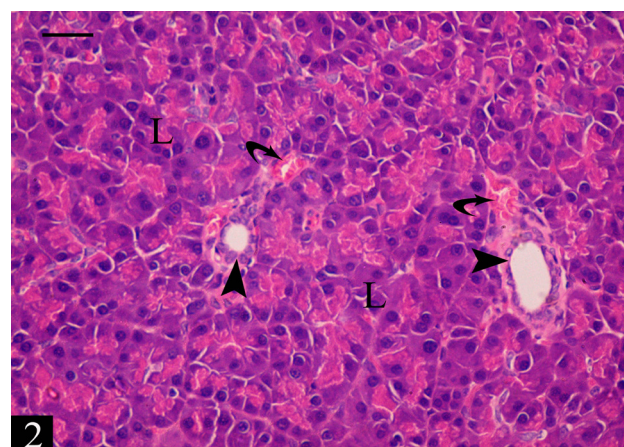


Fig. 2: showing variable sized interlobular ducts lined by cuboidal epithelium (arrow head) and blood vessels (curved arrow) in the thin connective tissue septa between the pancreatic lobules (L). (Group I, H&E X 400, Scale bar = 50µm)

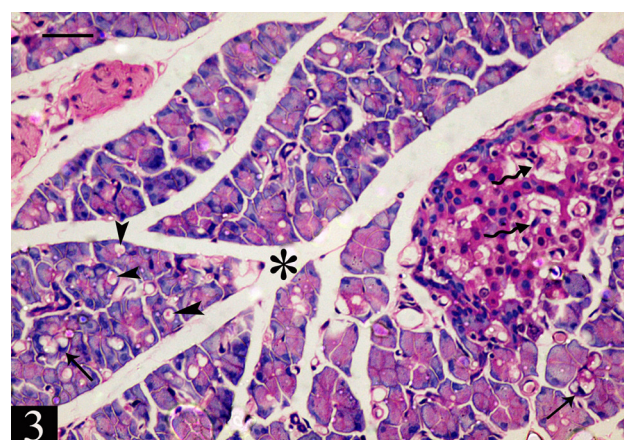


Fig. 3: showing cytoplasmic vacuolation and deeply stained pyknotic nuclei in many acinar (arrow) and islets cells (wavy arrow). Notice large autophagic vacuoles containing acidophilic material in some acinar cells (arrow head) and widely separated lobules (*). (Group II, H&E X 400, Scale bar = 50µm)

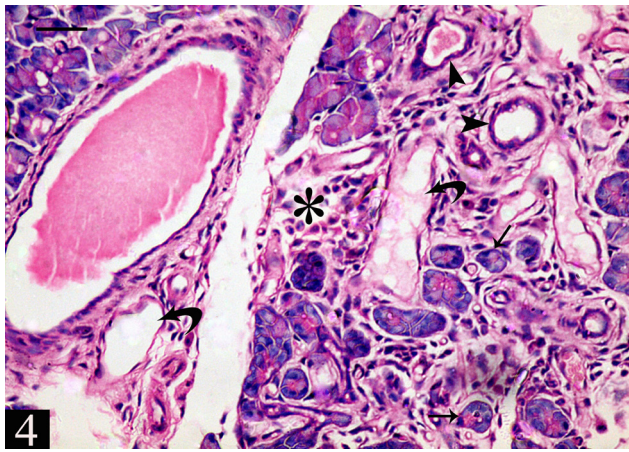


Fig. 4: showing disturbed architecture of a pancreatic lobule with an obvious distortion in its acini and heavy infiltration with mononuclear inflammatory cells (*). Notice apparent decrease in the size and number of the acini (arrow), dilated interlobular and intralobular ducts with retained secretion and flattening of their lining epithelium (arrow head) and markedly dilated blood vessels (curved arrow). (Group II, H&E X 400, Scale bar = 50µm)

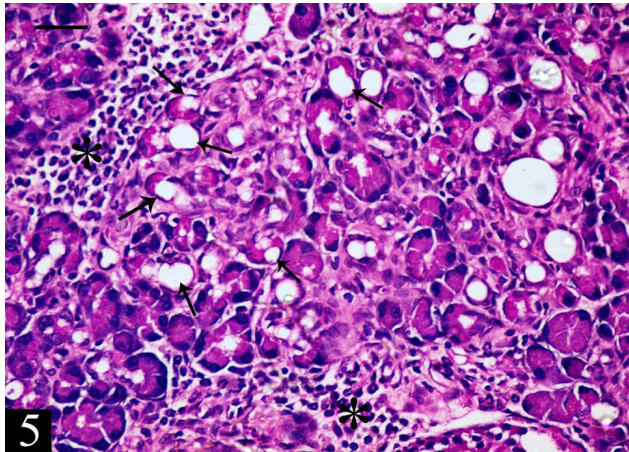


Fig. 5: showing large autophagic vacuoles in many acini (arrow) and heavy mononuclear cellular infiltration (*). (Group II, H&E X400, Scale bar = 50µm)

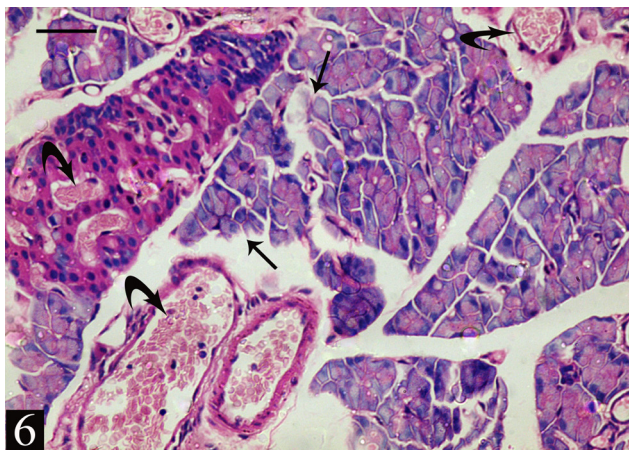


Fig. 6: showing markedly dilated and congested blood vessels (curved arrow). Notice destruction of some acini (arrow) and an apparent decrease in the apical acidophilia of the acinar cells. (Group II, H&E X 400, Scale bar = 50µm)

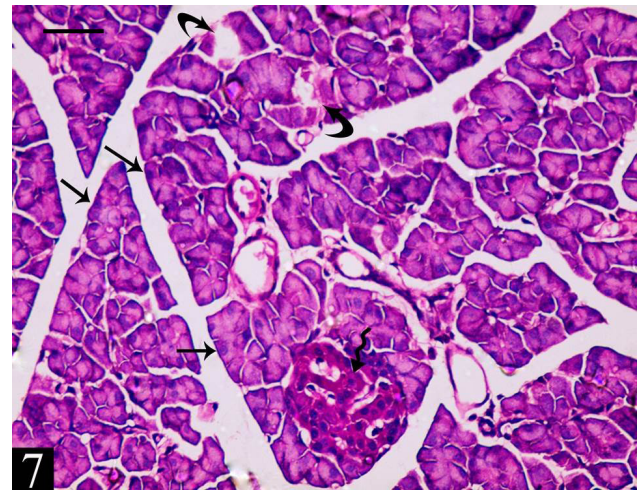


Fig. 7: showing preserved morphological structure of most acinar (arrow) and islets cells (wavy arrow). Notice a few damaged acini (curved arrow). (Group III, H&E X 400, Scale bar = 50µm)

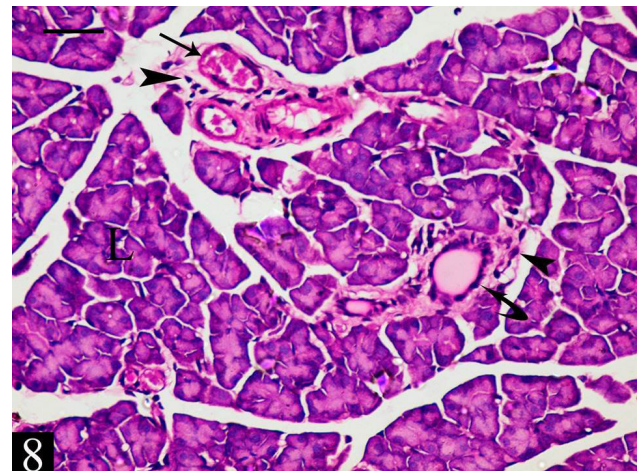


Fig. 8: showing preserved lobular architecture (L) with thin connective tissue septa, dilated intralobular duct (curved arrow) and mild dilatation and congestion of the blood vessels (arrow) with minimal cellular infiltration (arrow head). (Group III, H&E X 400, Scale bar = 50µm)

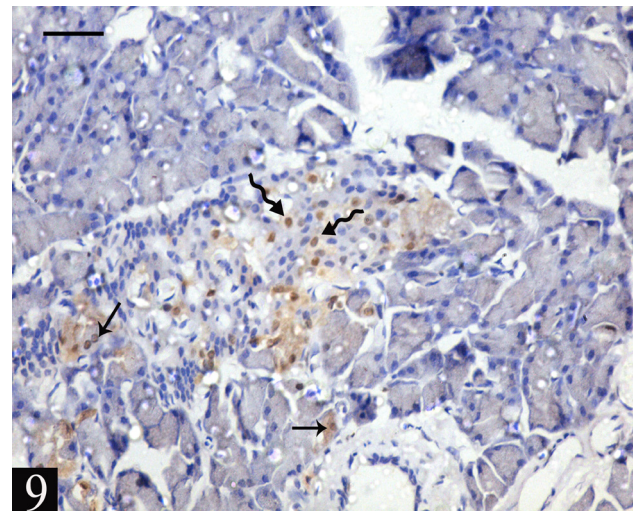


Fig. 9: showing a weak positive brown immunoreaction for P53 in nuclei of a few acinar (arrow) and islets cells (wavy arrow). (Group I, P53-immunostaining X 400, Scale bar = 50µm)

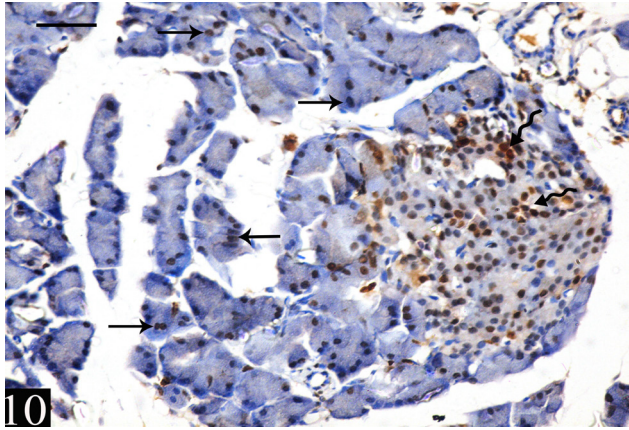


Fig. 10: showing a strong positive P53 immunoreaction in nuclei of many acinar (arrows) and islets cells (wavy arrow) (Group II, P53-immunostaining X 400, Scale bar = 50µm)

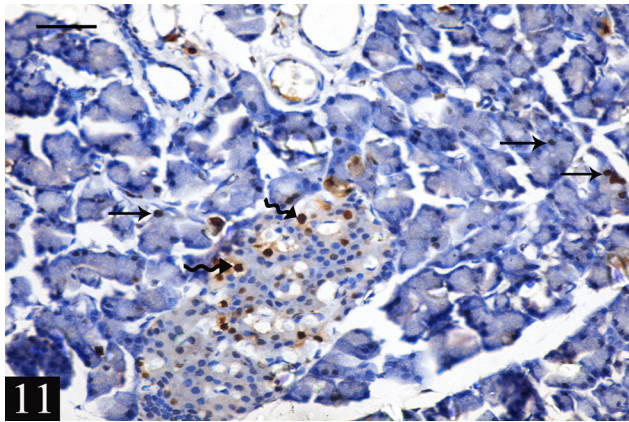


Fig. 11: showing a moderate positive immunoreaction for P53 in nuclei of some acinar (arrows) and islets cells (wavy arrow). (Group III, P53-immunostaining X 400, Scale bar = 50µm)

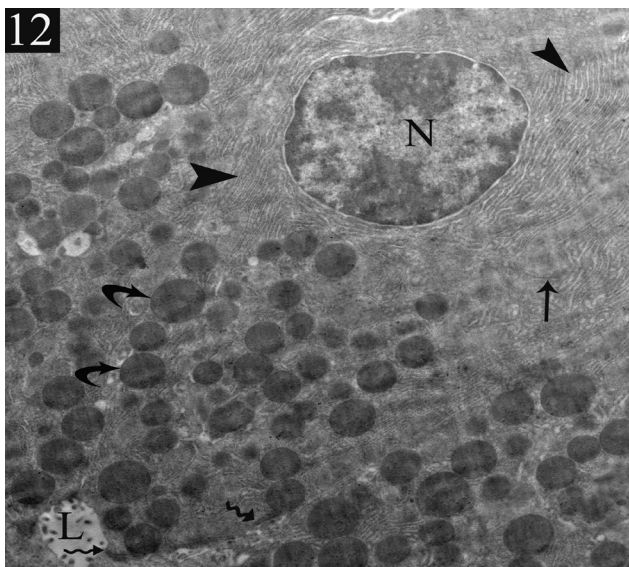


Fig. 12: An electron micrograph for an acinar cell showing apically located spherical electron dense granules (curved arrow) and basal rounded euchromatic nucleus (N) surrounded by parallel cisternae of rough endoplasmic reticulum (arrow head) and mitochondria (arrow). Notice a few microvilli in the lumen (L) of the acinus and the junctional complexes (wavy arrow) between its acinar cells. (Group I, X 11700)

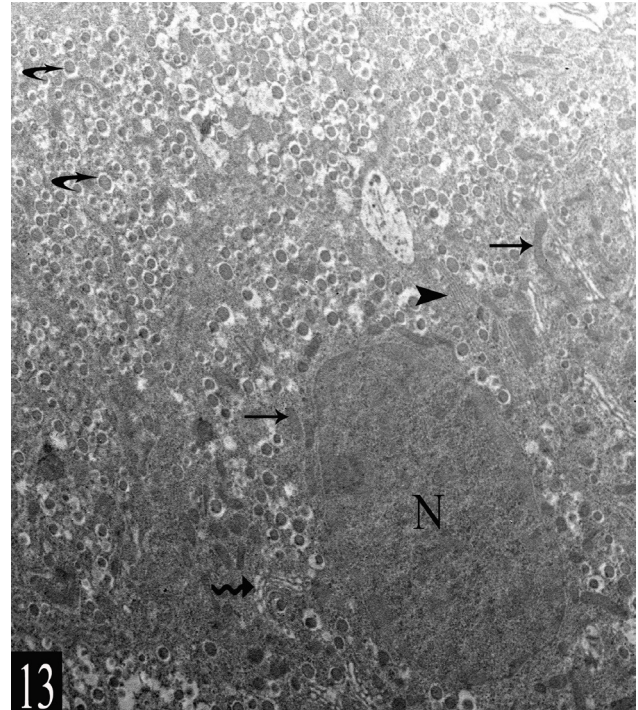


Fig. 13: An electron micrograph for a beta cell showing an ovoid regular euchromatic nucleus (N), numerous dense core granules bounded by a wide clear halo (curved arrow), multiple mitochondria (arrow), rough endoplasmic reticulum (arrow head) and Golgi apparatus (wavy arrow). (Group I, X 11700)

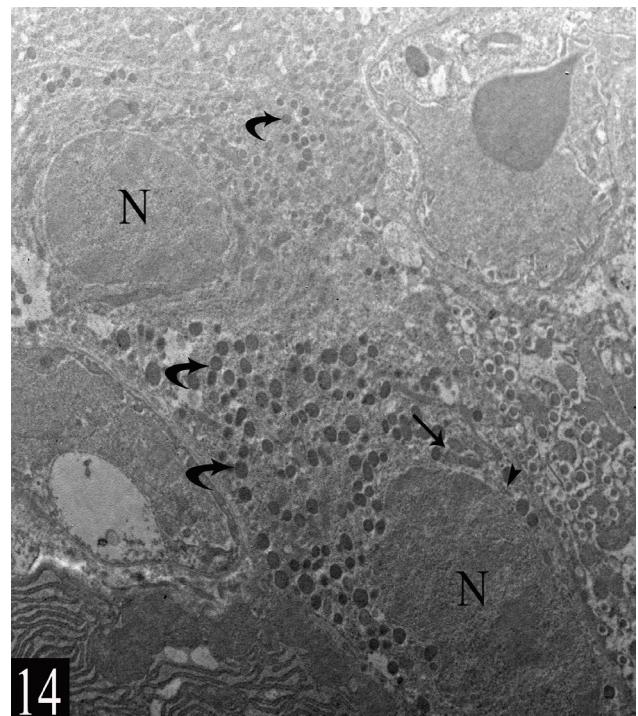


Fig. 14: An electron micrograph for alpha cells showing ovoid nuclei (N), numerous electron-dense granules (curved arrow), multiple mitochondria (arrow) and rough endoplasmic reticulum (arrow head). (Group I, X 11700)

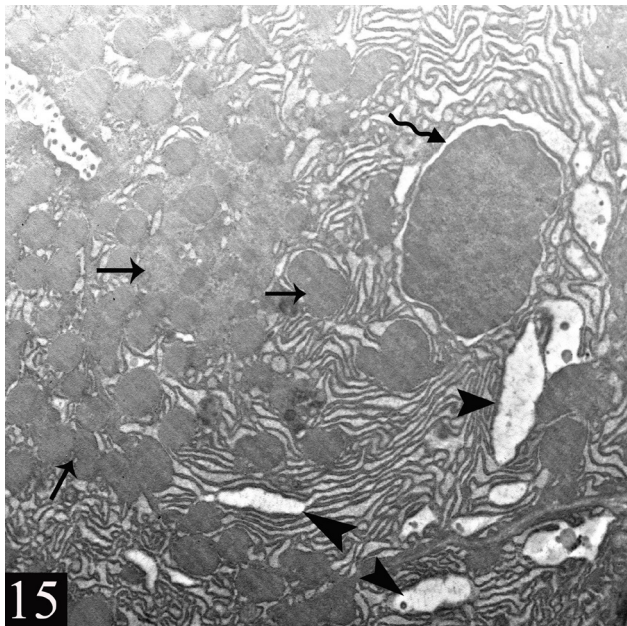


Fig. 15: An electron micrograph for an acinar cell showing dilated rough endoplasmic reticulum (arrow head) and dilated perinuclear space (wavy arrow). Notice fusion of the less electron-dense granules (arrow). (Group II, X 11700)

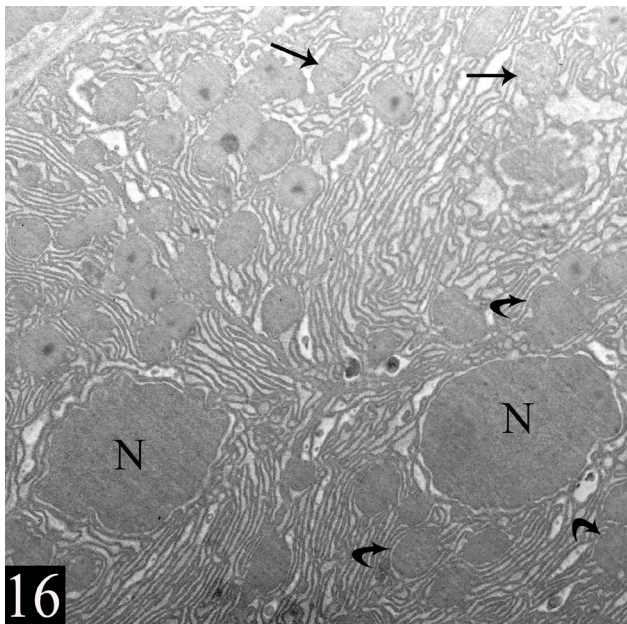


Fig. 16: An electron micrograph for acinar cells showing swollen mitochondria with disrupted cristae (arrow), shrunken irregular heterochromatic nuclei (N), abnormal distribution of the granules throughout the cytoplasm (curved arrow) and an apparent decrease in the number of the granules. (Group II, X 11700)

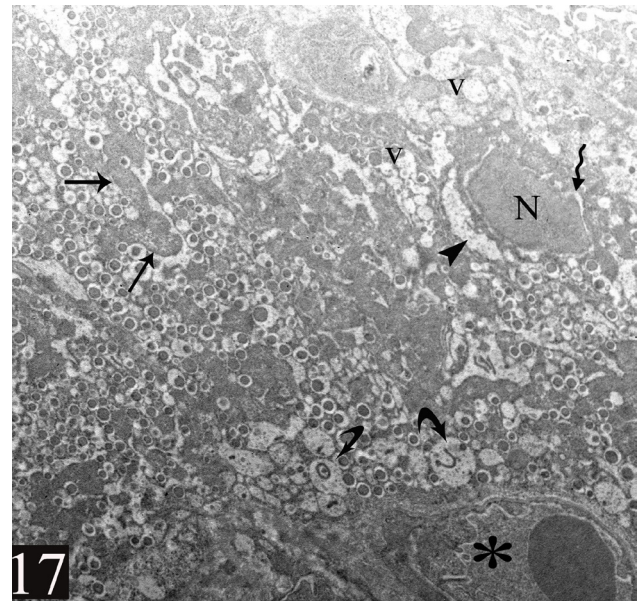


Fig. 17: An electron micrograph for beta cells showing cytoplasmic vacuoles (V), swollen disrupted mitochondria (arrow), dilated rough endoplasmic reticulum (arrow head), dilated perinuclear space (wavy arrow), numerous autophagic vacuoles (curved arrow) and a shrunken irregular heterochromatic nucleus (N). Notice the presence of a blood vessel between beta cells (*). (Group II, X 11700)

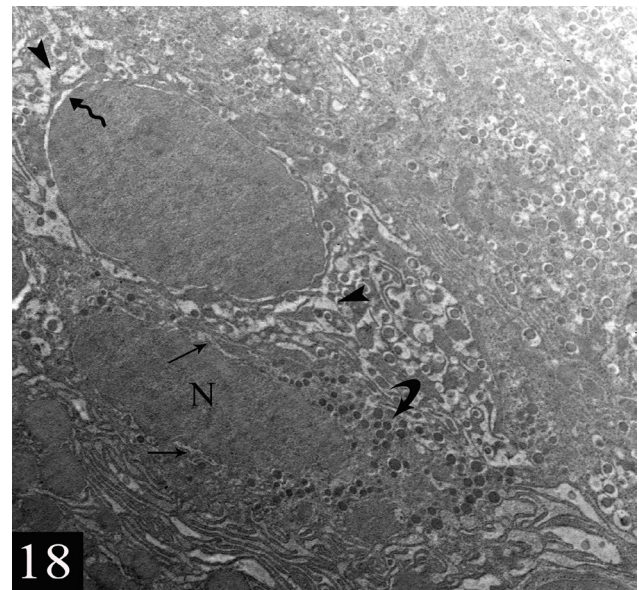


Fig. 18: An electron micrograph for an alpha cell showing an ovoid nucleus (N), rough endoplasmic reticulum (arrow) and numerous electron-dense granules (curved arrow) in the cytoplasm. Notice dilated perinuclear space (wavy arrow) and rough endoplasmic reticulum (arrow head) of the beta cell. (Group II, X 11700)

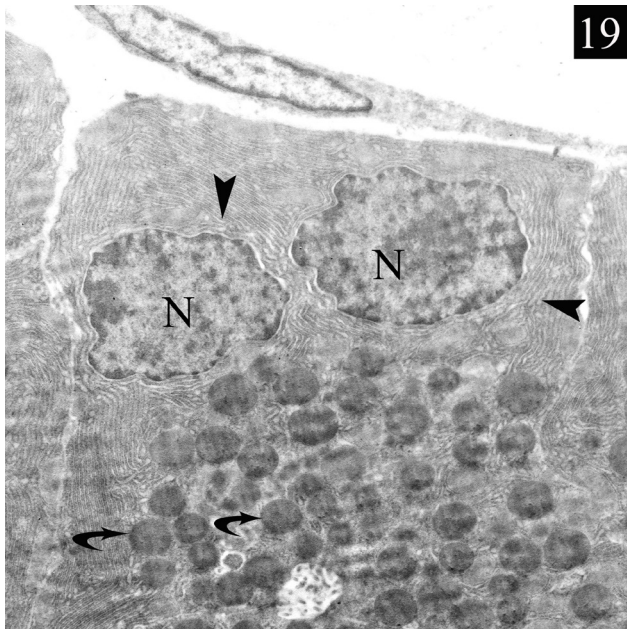


Fig. 19: An electron micrograph for an acinar cell showing apically located spherical electron dense granules (curved arrow) and basal euchromatic nuclei (N) surrounded by parallel cisternae of rough endoplasmic reticulum (arrow head). (Group III, X 11700)

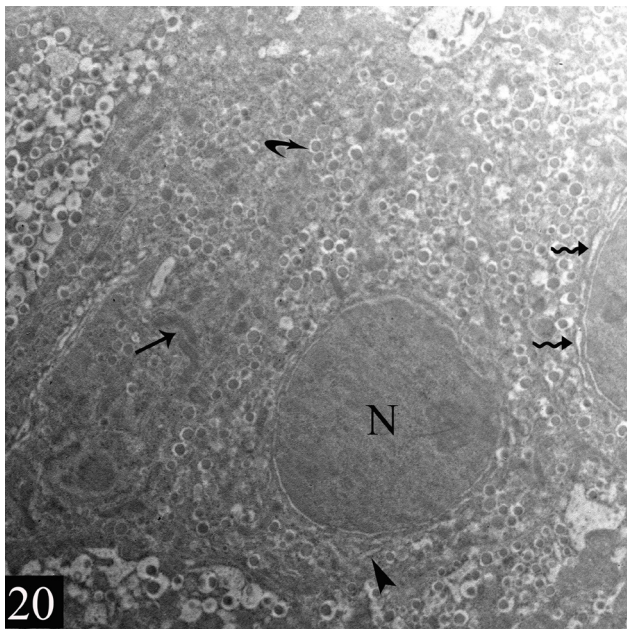


Fig. 20: An electron micrograph for a beta cell showing an ovoid regular euchromatic nucleus (N), numerous dense core granules bounded by a wide clear halo (curved arrow), multiple mitochondria (arrow) and rough endoplasmic reticulum (arrow head). Notice mild dilatation of rough endoplasmic reticulum of other beta cell (wavy arrow). (Group III, X 11700)

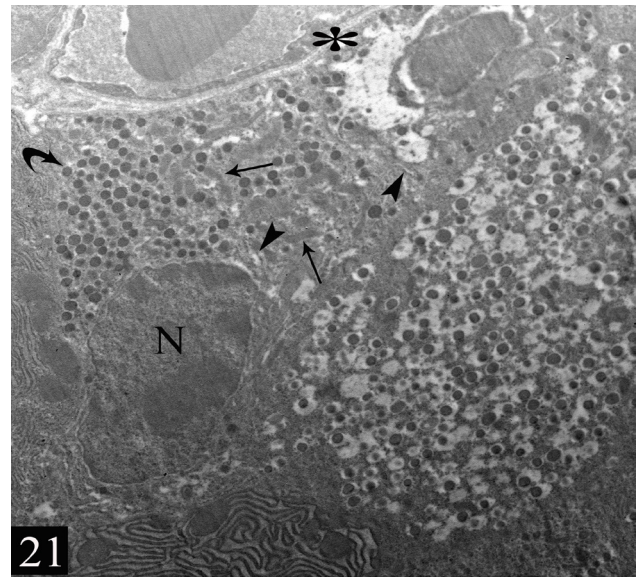
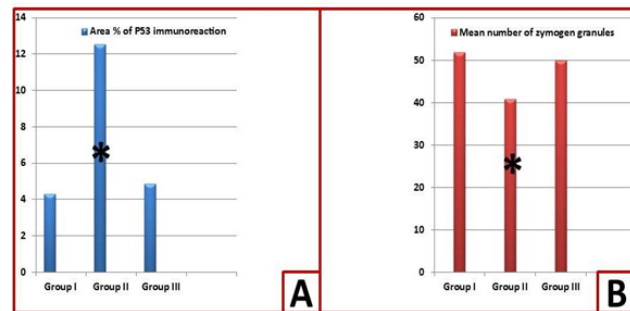


Fig. 21: An electron micrograph for beta and alpha cells. The alpha cell shows ovoid nuclei (N), numerous electron-dense granules (curved arrow), multiple mitochondria (arrow) and rough endoplasmic reticulum (arrow head). Notice the presence of blood vessels between cells (*). (Group III, X 11700)

Table 1: illustrates area % of P53 immunoreaction and number of zymogen granules (Mean ± SD)

Groups	Group I (control group)	Group II (valproic acid group)	Group III (valproic acid -marjoram group)
Parameters			
Mean area % of P53	4.289±0.723	12.53±1.74*	4.865±0.473
Mean number of zymogen granules	51.9±5.07	40.8±6.14*	49.9.59±4.12

*P < 0.05 is significant value versus group I



Histogram 1: Morphometrical & statistical analysis of (A) Mean area % of P53 positive immunoreaction. (B) Mean number of zymogen granules.* indicates significance vs control

DISCUSSION

Valproic acid is an antiepileptic drug that is extensively prescribed for many neurological disorders. Despite its effectiveness, its administration is associated with serious complications. The pancreas is a target organ that is affected by valproic acid administration leading to pancreatitis^[34,35]. Recently, several studies reported the health protective values of the marjoram oil due to its antioxidant activities^[36,37]. Accordingly, this research aimed to study the effect of valproic acid on the pancreas of adult male albino rat exploring novel mechanisms of VA-induced damage and to evaluate the potential protective effect of marjoram oil through various histological methods.

In this research, valproic acid administration to rats altered the histological structure of their pancreas. These changes included loss of the normal architecture of the lobules and an obvious distortion in the exocrine acini as well as the endocrine islets of Langerhans. The acinar and islets cells showed cytoplasmic vacuoles and pyknotic nuclei. Dilated ducts and blood vessels were seen. There was a significant increase in the P53-immunoreaction of the acinar and islets cells and a significant decrease in the number of the zymogen granules of the acinar cells. Ultrastructurally, there were shrunken heterochromatic nuclei with irregularity, dilated rough endoplasmic reticulum and perinuclear space and swollen disrupted mitochondria in the acinar cells and beta cells. These adverse findings of valproic acid administration were supported by some researchers who reported that valproic acid caused disturbance of the normal structure of the pancreas causing acute pancreatitis^[1,34].

Moreover, no significant ultrastructural changes were observed in alpha cells of VA-treated rats. It was reported that alpha cells are less reactive to injury compared to beta cells and display adaptation to cellular stress^[38]. Furthermore, recent studies demonstrated that in adult pancreas, beta cell injury by various etiologies might activate alpha cells to transdifferentiate into new beta cell replacing the lost ones. A paracrine/autocrine mechanism is proposed whereby beta cells injury causes the release of factors as stromal cell-derived factor-1 that induces the de-differentiation of the adjacent alpha cells into pro-alpha cells. The pro-alpha cells transdifferentiate into beta cells. The transdifferentiation of pro-alpha cells into beta cells provides a potentially exploitable mechanism for beta cells regeneration in adult pancreas^[39,40].

It was reported that VA caused elevated ROS levels and reduced tissue antioxidant capability in addition to increased lipid peroxidation and depletion of the glutathione. Lipid peroxidation due to oxygen free radicals was believed to be an important cause of damage and destruction of cell membranes. The high ROS levels are associated with the inflammatory response. Moreover, it induced mitochondrial dysfunction in VA-treated animals. So, the valproic acid induced injury and tissue damage is attributed to oxidative stress and mitochondrial dysfunction^[41].

Valproic acid induced acute pancreatitis that leads to a common pathway of changes in the pancreatic cells. These changes are intracellular activation of digestive enzymes with the appearance of cytosolic vacuoles, activation of NF- κ B, and release of pro-inflammatory cytokines. These changes are triggered by an abnormal rise in the cytosolic calcium level, which is dependent mainly on release of calcium from endoplasmic reticulum. The activated enzymes are directly damaging the cells in addition to recruitment of the circulating neutrophils resulting in further cellular damage. Neutrophil activation and cytokines lead to inflammatory response that is seen in severe acute pancreatitis^[42,43].

VA could interfere with cell cycle and cause DNA damage through inhibition of histone deacetylase activity. VA-induced DNA damage results in instability of RNA and protein synthesis. VA could induce endoplasmic reticulum [ER] stress as a mechanism of pancreatic damage^[15].

In this study, cytoplasmic vacuolation and small deeply stained nuclei were seen in many acinar and islets cells of VA-treated rats. This finding can be explained by being hydropic changes of the cytoplasm and nuclear degeneration which is manifested as pyknosis caused by oxidative stress^[44,45].

Mononuclear cell infiltration was observed in the damaged pancreatic areas of VA-treated rats. Valproic acid caused the release of soluble products such as monocyte chemo-attractant protine-1 stimulating mononuclear cell infiltration into the interstitium which differentiated into macrophages. These cells released proinflammatory cytokines such as IL-1 β and TNF- α leading to ROS production and tissue injury^[41].

The ultrastructural alteration of the mitochondria, rough endoplasmic reticulum and the nuclei were seen in the acinar and beta cells of VA-treated rats. These changes were attributed to increased free radicals production and decreased free radical scavenging. Valproic acid induced cytotoxicity through formation of oxygen radicals against the nuclear DNA. Also, cytotoxicity of VA is the result of generation of hydrogen peroxides and highly reactive hydroxyl radicals. In addition, it enhances the clearance of copper, selenium and zinc, subsequently resulting in decreased synthesis of free radicals scavenging enzymes as glutathione peroxidase and glutathione reductase. Furthermore, the cytotoxicity of VA may be due to lysosomal membrane leakiness along with ROS production^[46,28].

Moreover, numerous autophagosomes were also observed in VA-treated rats and this may be considered as a defense mechanism by which the body tries to maintain cell homeostasis and to prevent the occurrence of ER stress as well as maintaining the normal protein synthesis activity and secretion^[15]. In addition, the lysosomal and mitochondrial dysfunction in pancreatitis leads to ER stress, activation of trypsinogen and impaired autophagy. This impaired autophagy was manifested in our current study by accumulated large autophagic vacuoles containing

partially degraded material. Impaired autophagy resulted in inflammation and cell death. So, autophagy may be involved in the pathogenesis of VA-induced pancreatic damage^[47,48].

Moreover, an apparent decrease in the zymogen granules with abnormal cytosolic distribution was observed by E/M examination in VA-treated rats. This decrease in the number of the zymogen granules was also confirmed by the morphometric and statistical analysis. This finding is attributed to an abnormal rise in the cytosolic calcium level released from endoplasmic reticulum due to VA-induced acute pancreatitis. This leads to inhibition of secretion and zymogen activation and stimulates cell death mechanisms. Moreover, the E/M examination revealed abnormal distribution of the zymogen granules which is attributed to disruption of the actin cytoskeleton due to VA-induced pancreatitis resulting in dispersion of the granules throughout the cytoplasm. The actin cytoskeleton is responsible for the normal distribution of these granules to the apical cell domain. Also, the specific mechanism for blocking the basolateral membrane exocytosis is disrupted in acute pancreatitis^[49].

Immunohistochemically, our results revealed a significant increase in P53 immunoeexpression in VA-treated rats. P53 (a tumor suppressor protein) is a pro-apoptotic nuclear transcription factor that can activate genes of apoptosis after DNA damage. Therefore, the increased P53 expression upon VA administration may suggest DNA damage as a mechanism of VA-induced pancreatic damage. P53 is transferred to mitochondria causing the release of other pro-apoptotic agents like Bax and Fas. The increased P53 may also lead to reduced Bcl-2 which is an anti-apoptotic agent that prevents the mitochondrial liberation of the pro-apoptotic agents. This was attributed to the increase ROS accumulation and activation of the oxidizing enzymes by VA leading to mitochondrial damage and cell death^[28,50]. So, the increase in the expression of this apoptosis-related gene (P53) in the present study may explain a possible mechanism involved in VA-induced pancreatic damage.

In this study, marjoram oil was given to rats one hour before valproic acid to avoid herb/drug interaction^[51] and our results showed the protective value of marjoram oil against VA-induced pancreatic damage. This finding is supported by previous reports which stated that marjoram oil exerted its protective action through antioxidant and anti-inflammatory mechanisms. Marjoram oil is an excellent source for antioxidants as polyphenolic compounds, minerals and vitamins. Marjoram oil significantly attenuates lipid peroxidation and enhances the antioxidant enzymes^[52,53]. This antioxidant role was attributed mainly to the high content of rosmarinic acid, anthocyanins and tannin derivatives. It has also a potent peroxyl radical scavenging action to protect the biological membranes from free radicals. It neutralizes the elevated ROS to prevent DNA oxidative damage. Furthermore, the anti-inflammatory role of marjoram oil was attributed

to its high content of eugenol. In addition, terpineol and sabinene hydrate in marjoram oil could suppress tumor necrosis factor- α (TNF α), interleukin 1 β (IL-1 β), IL-6, and IL-10 inhibiting cyclooxygenase 2 (COX2) and NF κ B gene expression reducing tissue inflammation^[54,55]. It also attenuated apoptosis induced by gene expression which is attributed to its antioxidant effect^[56]. This anti apoptotic effect was proved in this work by the significant decrease in P53 immunoeexpression.

So, co-administration of marjoram oil to VA ameliorated all our study parameters and modulated the up-regulation in the expression level of P53. This is indicative of a protective interfering role against VA-induced pancreatic damage.

CONCLUSION AND RECOMMENDATIONS

This research showed that VA administration to albino rats changed the histological structure and induced apoptosis in the pancreas affecting mainly the acinar and beta cells. The study also revealed the possible participation of P53 (apoptosis-related gene) in the development of VA-induced pancreatic damage. The study suggests that marjoram oil might be beneficial in minimizing the pancreatic damage induced by VA through its anti-inflammatory, anti-oxidant and anti-apoptotic effects. Therefore, marjoram oil could be a promising protective agent for patients receiving VA minimizing its pancreatic complications. Further clinical studies on human are required to confirm the beneficial role of marjoram oil.

CONFLICT OF INTERESTS

There are no conflicts of interest.

REFERENCES

1. Oktay S, Alev-Tuzuner B, Tunali S, Ak E, Emekli-Alturfan E, Tunali-Akbay T, Koc-Ozturk L, Cetinel S, Yanardag R, Yarat A (2017). Investigation of the Effects of Edaravone on Valproic Acid Induced Tissue Damage in Pancreas. *Marmara Pharm J.*, 21: 570–577.
2. Huang W, Ren X, Shen F, Xing B (2019). Sodium valproate induced acute pancreatitis in a bipolar disorder patient: a case report. *BMC Pharmacol Toxicol.*, 20: 71.
3. Oztopu O, Turkon H, Buyuk B, Coskun O, Sehitoglu MH, Ovali MA, Uzun M (2020). Melatonin ameliorates sodium valproate induced hepatotoxicity in rats. *Molecular Biology Reports*, 47:317–325.
4. Okdah YA and Ibrahim S (2014). Effect of aqueous saffron extract (*Crocus sativus* L.) on sodium alproate-induced histological and histochemical alterations in liver of albino rats. *International Journal of Advanced Research*, 2(7): 735-745.
5. Al-Amoudi WA (2017). Protective effects of fennel oil extract against sodium valproate-induced hepatorenal damage in albino rats. *Saudi J Biol Sci.*, 24(4):915-924.

6. Lahneche AM, Boucheham R, Boubekri N, Bensaci S, Bicha S (2017). Sodium valproate-induced hepatic dysfunction in albino rats and protective role of n-Butanol extract of *Centaurea sphaerocephala* L. *International Journal of Pharmacognosy and Phytochemical Res.*, 9 (10): 1335-1343.
7. Morsy BM, Safwat GM, Hussein DA, Samy RM (2017). The protective effect of *Nigella sativa* oil extract against neurotoxicity induced by Valproic acid. *International Journal of Bioassays*, 6(9): 5474-5484.
8. Schwarz K, Romanski A, Puccetti E, Wietbrauk S, Vogel A, Keller M, Scott JW, Serve H, Bug G (2011). The deacetylase inhibitor LAQ824 induces notch signaling in hematopoietic progenitor cells. *Leuk Res.*, 35(1): 119-125.
9. Gad AM (2018). Study on the influence of caffeic acid against sodium valproate-induced nephrotoxicity in rats. *J Biochem Mol Toxicol.*, 32(8): e22175.
10. Iamsaard S, Sukhorum W, Arun S, Phunchago N, UabundiTN, Boonruangsri P, Namking M (2017). Valproic acid induces histologic changes and decreases androgen receptor levels of testis and epididymis in rats. *Int J Reprod Biomed.*, 15(4):217-224.
11. Jazayeri D, Braine E, McDonald S, Dworkin S, Powell KL, Griggs K, Vajda FJE, O'Brien TJ, Jones NC (2020). A rat model of valproate teratogenicity from chronic oral treatment during pregnancy. *Epilepsia*, 61(6):1291-1300.
12. Jones MR, Hall OM, Kaye AM, Kaye AD (2015). Drug-induced acute pancreatitis: a review. *Ochsner J.*, 15 (1):45-51.
13. Jain A, Haque I, Tayal V, Roy V (2019). Valproic acid-induced acute pancreatitis. *Indian J Psychiatry*, 61(4): 421-422.
14. Guseibat TA, Al-Sarraj KR, Elturshani OAM, El-nagaz EOM (2019). Effects of Valproic Acid on Pancreatic Tissues in Female Mice. *LJBS.*, 8 (1):26 – 37.
15. Ghoneim FM, Alrefai H, Elsamanoudy AZ, Abo El Khair SM, Khalaf HA (2020). The Protective Role of Prenatal Alpha Lipoic Acid Supplementation against Pancreatic Oxidative Damage in Offspring of Valproic Acid-Treated Rats: Histological and Molecular Study. *Biology (Basel)*, 9(9):239.
16. Aktas I, Gür FM, Özgöçmen M (2020). Silymarin Ameliorates Valproic Acid-Induced Pancreas Injury by Decreasing Oxidative Stress. *International Journal of Veterinary and Animal Research*, 3(2): 34-38.
17. Komariah k, Manalu W, Kiranadi B, Winarto A, Handharyani E, Roeslan MO (2018). Valproic Acid Exposure of Pregnant Rats During Organogenesis Disturbs Pancreas Development in Insulin Synthesis and Secretion of the Offspring. *Toxicol Res.*, 34(2): 173-182.
18. Wahby MM, Yacout G, Kandeel K, Awad D (2015). LPS-induced oxidative inflammation and hyperlipidemia in male rats: The protective role of *Origanum majorana* extract. *Beni-Suef University Journal of Basic and Applied Sciences*, 4 (4) 291-298.
19. Mansoury MMS (2019). Marjoram (*Origanum majorana* L.) Alleviate Myocardial Damage Induced by Doxorubicin in Rats. *J Biochem Tech.*, (4): 82-88.
20. El-Wakf AM, Elhabibi SM, AbdEl-Ghany E (2015). Preventing male infertility by marjoram and sage essential oils through modulating testicular lipid accumulation and androgens biosynthesis disruption in a rat model of dietary obesity. *Egyptian Journal of Basic and Applied Sciences*, 2 (3): 167-175.
21. Soliman MM, Abdo Nassan M, Ismail TA (2016). *Origanum majoranum* extract modulates gene expression, hepatic and renal changes in a rat model of type2. *Diabetes*, 15:45-54.
22. El-Meligy RM, Awaad AS, Soliman SA, Keawy SA, Alqasoumi SI (2017). Prophylactic and curative anti-ulcerogenic activity and the possible mechanisms of some desert plants. *Saudi Pharma J.*, 25:387-396.
23. Diab AA, Abdelsalam HM; Zahra MH, Eldehamy S, Hendawy BA (2019). Alleviative effects of marjoram and propolis against negative influences of adenine on renal and testicular efficiencies of male rats. *Int. J. Adv. Res. Biol. Sci.* 6(4): 194-207.
24. Pasavei AG, Mohebbati R, Boroumand N, Ghorbani A, Hosseini A, Jamshidi ST, Soukhtanloo M (2020). Anti-Hypolipidemic and Anti-Oxidative Effects of Hydroalcoholic Extract of *Origanum majorana* on the Hepatosteatosis Induced with High-Fat Diet in Rats. *Malays J Med Sci.*, 27(1): 57-69.
25. Moubarza G, Waggasb AM, Solimanc KM, Abd Elfatahd AA, Taha MM (2018). Effectiveness of aqueous extract of marjoram leaves in the treatment of aspartame liver toxicity. *Egyptian Pharmaceutical Journal*, 17 (3). 163-170.
26. Kamel MA (2014). Protective effects of Marjoram oil (*Organium Majorana* L.) on antioxidant enzymes in experimental diabetic rats. *Assiut Vet. Med. J.*, 60(140).
27. Abu Aita NA and Mohammed FF (2014). Effect of Marjoram Oil on the Clinicopathological, Cytogenetic and Histopathological Alterations Induced by Sodium Nitrite Toxicity in Rats. *Global Veterinaria*, 12 (5): 606-616.
28. El-Khateeb SA, Arafa MH, Ibraheem TR (2013). Influence of Silymarin on Valproic Acid Induced Hepatotoxicity in Adult Male Albino Rats. *Ain Shams J Forensic Med Clin Toxicol*, (20): 221-232.

29. Gaertner DJ, Hallman TM, Hankenson FC, Batchelder MA (2008). Anesthesia and analgesia for laboratory rodents. Anesthesia and analgesia in laboratory animals. 2nd edition. Academic press, San Diego, CA. Boston. 239-240.
30. Bancroft JD and Gamble M (2008). Theory and practice of histological techniques. 6th edition, Elsevier health science. 126-127.
31. Ramos-Vara JA, Kiupel M, Baszler T, Bliven L, Brodersen B, Chelack B, West K, Czub S, Del Piero F, Dial S, Ehrhart EJ, Graham T, Manning L, Paulsen D and Valli VE (2008). Suggested guidelines for immunohistochemical techniques in veterinary diagnostic laboratories. J Vet Diagn Invest., 20: 393–413.
32. Bozzola JJ and Russell LD (1999). Electron microscopy: principles and techniques for biologists, 2nd edition, Jones and Bartlett Publishers. 100-124.
33. Dawson-Saunders B and Trapp R (2001). Basic and clinical biostatistics. 3rd ed., Lang Medical Book, McGraw Hill Medical Publishing Division. 161-218.
34. Deschenes P, Autmizguine J, Major P, Kleiber N (2020): Valproic acid induced pancreatitis presenting with decreased level of consciousness in a child with tuberous sclerosis complex. J Pediatr Pharmacol Ther., 25(3): 256–260.
35. Pawlowska-Kamieniak A, Krawiec P, Pac-Kozuchowska E (2021): Acute pancreatitis as a complication of antiepileptic treatment: case series and review of the literature. Pediatr Rep., 13: 98-103.
36. Lahreche T, Bradaie ML, Hamdi TM (2020): In *Vitro* Assessment of Antioxidant Activity, Total Phenolic and Flavonoid Contents of Sweet Marjoram (*Origanum majorana* L.) Extract. International journal of Horticulture, Agriculture and Food science (IJHAF) 4(4):158-163.
37. Ennaji H, Chahid D, Aitssi S, Badou A, Khlil N, *et al.* (2020): Phytochemicals screening, cytotoxicity and antioxidant activity of the *Origanum majorana* growing in Casablanca, Morocco. Open J Biol Sci 5(1): 053-059.
38. Dusaulcy R, Handgraaf S, Visentin F, Howald C, Dermitzakis ET, Philippe J, *et al.* (2019): High-fat diet impacts more changes in beta-cell compared to alpha-cell transcriptome. PloS ONE 14(3): e0213299.
39. Habener JF and Stanojevic V (2012): α -cell role in β -cell generation and regeneration. Islets 4:3, 188-198.
40. Lafferty RA, Tanday N, Moffett RC, Reimann F, Gribble FM, Flatt PR and Irwin N (2021): Positive Effects of NPY1 Receptor Activation on Islet Structure Are Driven by Pancreatic Alpha- and Beta-Cell Transdifferentiation in Diabetic Mice. Front. Endocrinol. 12:633625.
41. Hamouda MHMA, Abdel Aal FS, El-Mashad FHY (2019): Effect of sodium valproate on the structure of the renal cortex of adult male albino rat and the role of cinnamon. Al-Azhar Med J 48(1): 1-28.
42. Raraty MGT, Murphy JA, Mcloughlin E, Smith D, Criddle D, Sutton R (2005): Mechanisms of acinar cell injury in acute pancreatitis. Scandinavian Journal of Surgery 94: 89–96.
43. Demirtas E, Korkmaz I, ğlu KC, Ayan M, Demirtas E, Yurtbay S, Yıldız E, Aydın U, Szarpak L (2020): Serum TLR9 and NF-Kb biochemical markers in patients with acute pancreatitis on admission. Emergency Medicine International Volume 2020, Article ID 1264714, 1-6.
44. Jassim AM (2013): Protective Effect of *Petroselinum crispum* (parsley) extract on histopathological changes in liver, kidney and pancreas induced by Sodium Valproate in male Rats. Kufa Journal For Veterinary Medical Sciences, 4 (1): 20-27.
45. Galaly SR, Abdella EM, Mohammed HM, khadrawy SM (2014): Effects of royal jelly on genotoxicity and nephrotoxicity induced by valproic acid in albino mice. Beni – Suef University Journal of basic and applied sciences, 31 -15.
46. Pourahmad, J.; Eskandari, M.R.; Kaghazi, A. and Shaki, F. (2012): A new approach on valproic acid-induced hepatotoxicity: involvement of lysosomal membrane leakiness and cellular proteolysis. Toxicol in *Vitro*, 26: 545–551.
47. Biczó G, Vegh ET, Shalbueva N, Mareninova OA, Elperin J, Lotshaw E, Gretler S, Aurelia Lugea A, Malla SR, Dawson D, Ruchala P, Whitelegge J, French SW, Wen L, Husain SZ, Gorelick FS, Hegyi P, Rakonczay Z, Gukovsky I, Gukovskaya AS (2018): Mitochondrial dysfunction, through impaired autophagy, leads to endoplasmic reticulum stress, deregulated lipid metabolism, and pancreatitis in animal models. Gastroenterology 154(3):689-703.
48. Yuan X, Wu J, Guo X, Li W, Luo C, Li S, Wang B, Tang L, Sum H (2021): Autophagy in acute pancreatitis organelle interaction and micro RNA regulation. Oxidative Medicine and Cellular longevity 2021(11); 1-12.
49. Gorelick FS and Thrower E (2009): The acinar cell and early pancreatitis responses. Clin Gastroenterol Hepatol. 7(11 Suppl): S10–S14.
50. Chen X, Wong P, Radany E, Wong JYC (2009): HDAC Inhibitor, Valproic Acid, Induces p53-Dependent Radiosensitization of Colon Cancer Cells. Cancer Biother Radiopharm., 24(6): 689–699.
51. Amadi CN and Mgbahurike aa (2018): Selected food/herb-drug interactions: Mechanisms and clinical relevance. Am J Ther., 25(4):e423-e433.

52. Muqaddas, Khera RA, Nadeem F, Jilani MJ (2016): Essential Chemical Constituents and Medicinal Uses of Marjoram (*Origanum majorana* L.) – A Comprehensive Review. *IJCBS.*, 9: 56-62.
53. Saleh NS, Allam TS, El-Rabeaie RM, El- Sabbagh HS (2018): Protective effect of some Egyptian medicinal plants against oxidative stress in rats. *AJVS.*, 58(1):1-14.
54. Bina F and Rahimi R (2017): Sweet marjoram: a review of ethnopharmacology, phytochemistry, and biological activities. *J Evid Based Complementary Altern Med.*, 22(1): 175–185.
55. Bouyahya A, Chamkhi I, Benali T, Guaouguaou F, Balahbib A, El Omari N, Taha D, Belmehdi O, Ghokhan Z, (2021): Traditional use, phytochemistry, toxicology, and pharmacology of *Origanum majorana* L. *Journal of Ethnopharmacology* 265,113318.
56. TM Heikal (2015): Antioxidant potentials of *Origanum majorana* leaves extract against reproductive toxicity and apoptosis-related gene expression resulted from methomyl exposure in male rat. *Planta Med* 81(16).

الملخص العربي

زيت البردقوش يخفف من تلف البنكرياس المحدث بحامض الفالبرويك في ذكور الجرذان البيضاء البالغة: دراسة هستولوجية وهستوكيميائية مناعية

أميرة عدلى كساب، هبة شرف الدين، أمل على عبد الحافظ

قسم الهستولوجيا وبيولوجيا الخلايا - كلية الطب - جامعة طنطا - مصر

المقدمة: حامض الفالبرويك هو دواء مضاد للصرع يوصف على نطاق واسع للعديد من الاضطرابات العصبية. يرتبط استخدامه بمضاعفات خطيرة في البنكرياس. زيت البردقوش هو عامل وقائي للصحة له نشاطا مثبتا كمضاد للأكسدة. **الهدف من البحث:** دراسة تأثير حامض الفالبرويك على بنكرياس ذكور الجرذان البيضاء البالغة وإستكشاف آليات جديدة مسببة لتلف البنكرياس الناجم عن حامض الفالبرويك و تقييم الدور الوقائي المحتمل لزيت البردقوش. **مواد وطرق البحث:** تم استخدام خمسون جرذاً من ذكور الجرذان البيضاء كمجموعة ضابطة ,ومجموعة حامض الفالبرويك ,ومجموعة حامض الفالبرويك و زيت البردقوش. تم إعطاء كل من حامض الفالبرويك (٢٠٠ مجم / كجم) وزيت البردقوش (٥,٥ مل / كجم) مرة واحدة يومياً عن طريق الفم لمدة ثمانية أسابيع. ، تم تجهيز عينات من البنكرياس للدراسة بالمجهر الضوئي والالكترونى, وقد أجريت دراسة هستوكيميائية مناعية باستخدام الأجسام المضادة لل (بي٥٣).

النتائج: أظهرت عينات من مجموعة حامض الفالبرويك تشويهاً واضحاً في حويصلات البنكرياس وكذلك جزر لانجرهانز. أظهرت خلايا الحويصلات وخلايا الجزر تجاويف بالسيتوبلازم وتغيرات بأنوية الخلايا. ظهرت فجوات كبيرة ذاتية البلعمة تحتوي على مادة محبة للحموضة في العديد من الخلايا. شوهدت القنوات والأوعية الدموية متضخمة. وكان هناك زيادة ذات دلالة احصائية في التفاعل المناعي لل [بي٥٣] في خلايا الحويصلات والجزر ونقص في حبيبات زيموجين لخلايا الحويصلات. أظهر الفحص المجهرى الالكترونى وجود أنوية منكمشة وغير منتظمة واتساع فى الشبكة اللاندوبلازمية الخشنة و تورم الميتوكوندريا فى خلايا الحويصلات وخلايا بيتا. فى المقابل ، حدثت تغييرات طفيفة فى مجموعة حامض الفالبرويك - البردقوش التى تلقت زيت البردقوش قبل حامض الفالبرويك. **الاستنتاج:** إعطاء حامض الفالبرويك للجرذان البيضاء سبب تغييرات تركيبية فى البنكرياس. زيت البردقوش خفف من آثار حامض الفالبرويك وحافظ على تركيب البنكرياس.